Synthesis and Optical Properties of Au-Ag Alloy Nanoclusters with Controlled Composition

J. F. Sánchez-Ramírez,[1,3] U. Pal,[2*] L. Nolasco-Hernández,[1] J. Mendoza Álvarez,[3] and J. A. Pescador-Rojas[1]

[1] CICATA-IPN, Legaría 694, Col. Irrigación, 11500 Mexico D. F., Mexico. e-mail: jfsanchez@ipn.mx
[2] Instituto de Fisica, Universidad Autonoma de Puebla, Apdo. Postal J-48, Puebla, Pue. 72570, Mexico.
[3] Departamento de Física, CINVESTAV-IPN, Apdo. Postal 14-740, 07000 Mexico D. F., Mexico.

Keywords: *Metal Nanoparticles, Binary alloy, Optical properties*

Abstract

Colloidal solid-solution-like Au-Ag alloy nanoclusters of different compositions were synthesized through citrate reduction of mixed metal ions of low concentrations, without using any other protective or capping agent. Optical absorption of the alloy nanoclusters was studied both theoretically and experimentally. The position of the surface plasmon resonance (SPR) absorption band of the nanoclusters could be tuned from 419 nm to 521 nm through the variation of their composition. Considering effective dielectric constant of the alloy, optical absorption spectra for the nanoclusters were calculated using Mie theory, and compared with the experimentally obtained spectra. Theoretically obtained optical spectra resembled well with the experimental spectra when the true size distribution of the nanoparticles were considered. High resolution transmission electron microscopy (HREM), high angle annular dark filed (HAADF) imaging and energy dispersive spectroscopy (EDS) revealed the true alloy nature of the nanoparticles with nominal composition preserved. The synthesis technique can be extended to other bimetallic alloy nanoclusters containing Ag.

*Corresponding author; E-mail: upal@sirio.ifuap.buap.mx, Fax: +52-222-2295611

1. Introduction

Recently, much attention has been paid to the synthesis and characterization of bimetallic nanoparticles due to their unique catalytic, electronic, optical, structural and thermal properties [1-5] and subsequent technological applications such as catalysts, sensors, nanoelectronic devices [6-13] and biosensors [14]. The properties and hence the applicability of these nanoparticles not only depend on their size and shape, but also on the combination of the component metals (composition) and their fine structure, either as alloy or as a core-shell structures. Bimetallic nanoparticles particularly with well-defined alloy structures of noble metals like Pt-Ru, Cu-Pd, Pt-Mo, Pt-W, Pt-Ni, Au-Ag provide practical examples for the influence of metal composition and their structures on their catalytic properties [15-19]. Au-Ag nanoparticles of alloy type structure exhibit high catalytic activities for low-temperature CO oxidation [18, 20] and aerobic oxidation of alcohol [21].

On the other hand, Au-Ag bimetallic nanoparticles show different optical responses for alloy and core-shell configurations, even when they have same Au and Ag contents. Au-Ag alloy nanoparticles show a single, composition-sensitive absorption band located at an intermediate position between pure Au and Ag nanoparticles surface plasmon resonance (SPR) peaks, which results in amplification of light-induced processes (*e.g.* Raman scattering) undergone by molecules localized on their surfaces, giving rise to surface-enhanced Raman scattering [22]. Thus the control of structural type and composition of bimetallic nanoparticles comprised of Ag and Au have been a subject of considerable interest; and the developed of simple and versatile methods for controlling the composition and structure of Au-Ag nanoparticles is an important and challenging task.

Bimetallic Au-Ag nanoparticles have been obtained using different synthesis methods including replacement reaction [23], biosynthesis [24], green synthesis methods [25], laser-assisted [26], alcohol reduction [27], borohydride reduction [28], laser ablation [29], ultrasound irradiation [30] and metal evaporation-condensation [31]. However, relatively few methods produce true alloy nanoparticles due to phase separation at the atomic level leading to the formation of core-shell particles [32-36].

We have succeeded in synthesizing true Au-Ag alloy nanoparticles of varying Au/Ag molar ratios in water, by slightly modifying the citrate reduction method used by Link et al. [37]. Optical and structural properties of the samples were studied using optical absorption spectroscopy in the UV-Vis range, transmission electron microscopy (TEM), high resolution TEM (HREM), and high angle annular dark field (HAADF) imaging techniques. Considering effective dielectric constant of the alloy, optical absorption spectra for the nanoclusters were calculated using Mie theory, and compared with the experimentally obtained spectra.

2. Experimental and theoretical calculations

Synthesis

Colloidal dispersions of bimetallic Au-Ag nanoparticles of different molar ratios were synthesized with a slight modification of conventional citrate reduction method without using any organic stabilizer. Typically, the method of citrate reduction involves concentrated solutions of metallic salts like $HAuCl_{4(s)}$ and $AgNO_{3(s)}$ and their simultaneous reduction with sodium citrate. However, the presence of high concentration Cl^- ions produced from the reduction of $HAuCl_4$ does not permit a complete dissolution of silver salts and therefore reduction of Ag^+ ions due to spontaneous formation of $AgCl_{(s)}$. Considering the solubility product (K_{ps}) of $AgCl_{(s)}$ (1.8×10^{-10}), to produce complete solubility of $AgNO_3$, it is necessary to use its solutions of concentrations

lower than the (K_{ps}) of $AgCl_{(s)}$ [38]. To verify this criterion, we prepared two sets of metal ion solutions with different concentrations. In the first set, gold and silver ion solutions of 1.32 mM concentrations were prepared by dissolving $HAuCl_{4(s)}$ and $AgNO_{3(s)}$ in water, respectively. In the second set, metal ion solutions of 1.32 x 10 $^{-3}$ mM were prepared in a similar way. Both the solutions were mixed at room temperature at various Au/Ag molar ratios (= 9/1, 3/1, 1/1, 3/1, 1/9) to make a total volume of 25 ml of bimetallic ion mixture. While for the first batch of ionic solutions the solubility product was above the solubility product (K_{ps}) of $AgCl_{(s)}$, in the latter batch, the solubility product was below the (K_{ps}) of $AgCl_{(s)}$. To reduce the metal ions, 1 ml aqueous solution of sodium citrate (3.5 x 10^{-5} m mol in 5 ml of H_2O) was added to the mixture solutions at 100 °C temperature under magnetic agitation and refluxed for 1 h. The same procedure was followed to prepare the monometallic Au and Ag colloids. Homogeneous colloidal dispersions were formed after the addition of reductor in the metal ion solutions. On adding the reductor, the color of the $HAuCl_4$ solution changed from clear yellow to red. In contrast, the $AgNO_3$ solution changed from colorless to light yellow. The intermediate compositions resulted in colors that are varying between yellow and red. While the colloidal solutions prepared with the first batch of solutions (with high metal ion concentrations) did precipitate after a couple of days, we did not observe any flocculation or precipitation for the second batch of samples (prepared with very low concentration of metal ions) even after a couple of months.

Characterizations

Room temperature optical absorption spectra of the colloidal samples were recorded using a 10 mm path length quartz cuvette in a UV-Vis-NIR scanning spectrophotometer (Shimadzu UV 3101PC double beam). For transmission electron microscopic (TEM) observations, a drop of

colloidal solution was spread on a carbon coated copper micro-grid and dried in vacuum. For electron microscopy analysis, two microscopes, a Jeol JEM200 and a Tecnai 200 TEM with field-emission gun by FEI, were used for the low magnification and high-resolution observation of the samples, respectively. High-resolution electron microscope (HREM) images were digitally processed by using filters in the Fourier space. HAADF images were recorded with a Jeol 2010F microscope in the STEM mode, with the use of a dark field detector. Energy dispersive spectroscopy of the samples was performed using a Jeol JSM6390 scanning electron microscope with NORAN analytical system attached.

Theoretical calculations

Formal solutions of the phenomena of light absorption and scattering by small metal particles are obtained using Mie theory [39-41]. The physical effect of light absorption by the metallic nanoparticles suspended in liquids is the coherent oscillation of conduction band electrons (SPR) through the interaction with electromagnetic filed, where the electronic transitions between the associated discrete energies give the extinction (absorption + diffusion) of a part of incident light resulting a coloring effect in these systems. The absorption and dispersion of light in nanoparticles depend on the nature of the metal, along with their chemical composition, morphology and sizes. In the case of spherical nanoparticles separated by long distance, with no substance adsorbed on their surfaces, their absorbance, *A,* can be calculated as:

$$A = lC_{ext}\frac{C_{Au_xAg_{x-1}}}{fr^3} \qquad (1),$$

where r is the particle radius, C_{ext} is the extinction cross section for a single particle in nm^2, l is the optical path length in nm, $C_{Au_xAg_{x-1}}$ is the concentration of the alloy Au_xAg_{x-1} in g cm^{-3}, and f is a constant which depends on the average bulk density ρ of the alloy, and given by:

$$f = \frac{4\pi\rho}{3} \qquad (2).$$

In table 1, the concentrations of each of the alloy clusters used for our calculations and corresponding f values in g cm^{-3} are presented.

Table 1: Concentrations, f values and bulk free electron gas parameters for Au/Ag alloys of different compositions.

Molar ratio of Au and Ag	$C_{Au_xAg_{x-1}} \times 10^{-4}$ $(g\,cm^{-3})$	f (g cm^{-3})	v_f x10^6 (m s^{-1})	ω_d x10^{13} (s^{-1})	ω_p x 10^{16} (s^{-1})
1/0	2.600	186.183	1.390	3.225	1.350
9/1	2.482	177.684	1.390	3.170	1.352
3/1	2.306	164.936	1.390	3.086	1.355
1/1	2.012	143.689	1.390	2.948	1.360
1/3	1.718	122.442	1.390	2.809	1.365
1/9	1.541	109.694	1.390	2.726	1.368
0/1	1.424	101.195	1.390	2.670	1.370

The extinction cross section of spherical particles embedded in a medium of refractive index N can be calculated by:

$$C_{ext} = 2\frac{\pi}{k^2}\sum_{n=1}^{\infty}(2n+1)\Re(a_n + b_n) \quad (3),$$

where $k = 2\pi N / \lambda$; $\Re$ is the real part of the sum of the scattering coefficients a_n and b_n, and are function of particle radius, and light wavelength λ (in terms of the Ricatti-Bessel functions). As the absorption band of noble metal nanoparticles is dominated by the free electron behavior, the dielectric function can be described well through the Drude´s model. The magnitudes of the real and imaginary parts of the dielectric function of the particles are affected when the particle size is smaller than the mean free path of the conduction electrons. Considering this size dependence and based on the Drude´s model, size dependent dielectric functions such as the damping frequency of the particle ω_r can be calculated using the relation [39, 40]:

$$\omega_r = \omega_d + B\frac{v_f}{r} \quad (4),$$

where v_f is the electron speed at the Fermi level (Table 1), ω_d is the bulk alloy damping constant (Table 1), and B is a theory-dependent factor, close to one [39].

The bulk dielectric function $\varepsilon(\omega) = \varepsilon_1(\omega) + i\varepsilon_2(\omega)$ for bimetallic systems $Au_xAg_{(1-x)}$ can be defined by considering the weighted average for each component:

$$\varepsilon_{av}(Au_x Ag_{(1-x)}) = \varepsilon_{av}(x,\omega) = x\varepsilon(Au) + x\varepsilon(Ag) \quad (5),$$

where x is the volume fraction of one component. The size dependent dielectric functions of the alloy nanoclusters can be expressed considering Drude model, as:

$$\varepsilon'(\omega,r) = \varepsilon'_{bulk} + \frac{\omega_p^2}{\left(\omega^2 + \omega_d^2\right)} - \frac{\omega_p^2}{\left(\omega^2 + \omega_r^2\right)} \quad (6)$$

$$\varepsilon''(\omega,r) = \varepsilon''_{bulk} + \frac{i\omega_p^2\omega_r}{\left[\omega\left(\omega^2 + \omega_r^2\right)\right]} - \frac{i\omega_p^2\omega_d}{\left[\omega\left(\omega^2 + \omega_d^2\right)\right]} \quad (7),$$

where ω, ω_p and ω_d are the light frequency, plasmon frequency of the bimetallic Au-Ag alloy, and bulk alloy damping constant, respectively.

For calculations, a modified Mie program developed by Kreibing and Vollmer [39] and compiled in Fortan 77, was utilized. For this purpose, wavelength dependent refractive indices of gold and silver [42] were included in the data bank of the MieCalc program [43]. A fixed refractive index value (1.33) [44] of water was used in the calculations. For calculating the optical absorption spectrum of each bimetallic colloid, corresponding experimentally obtained size distribution histogram (Fig. 4) was used. First, the whole size distribution histogram was divided into several equal size ranges. For each size range, corresponding average particle size was used for calculation of absorption spectrum. On obtaining the absorption spectrum for each of the size ranges, the final absorption spectrum of the sample was obtained by considering the normalized fraction of particles as the weighted average of the corresponding sectional

absorption spectrum. Throughout the calculation, the true metal concentrations of the colloids were considered.

3. Results and Discussion

Nanoparticles of noble metals such as gold and silver in the size scale smaller than wavelengths of visible light strongly scatter and absorb light due to surface plasmon resonance (SPR, collective oscillation of conduction electron induced by incident light). The frequency and intensity of SPR band depend on the size, shape, structure and composition [39,40,45] of the metal nanoparticles. While the techniques like TEM, HREM reveal the exact size and shape of those nanoparticles, optical absorption spectra give a quick and gross idea on their shapes and sizes. In this study we used TEM, HREM and HAADF, along with optical absorption spectroscopy to study the size, size distribution, fine structure and composition homogeneity of bimetallic Au/Ag colloids of different compositions.

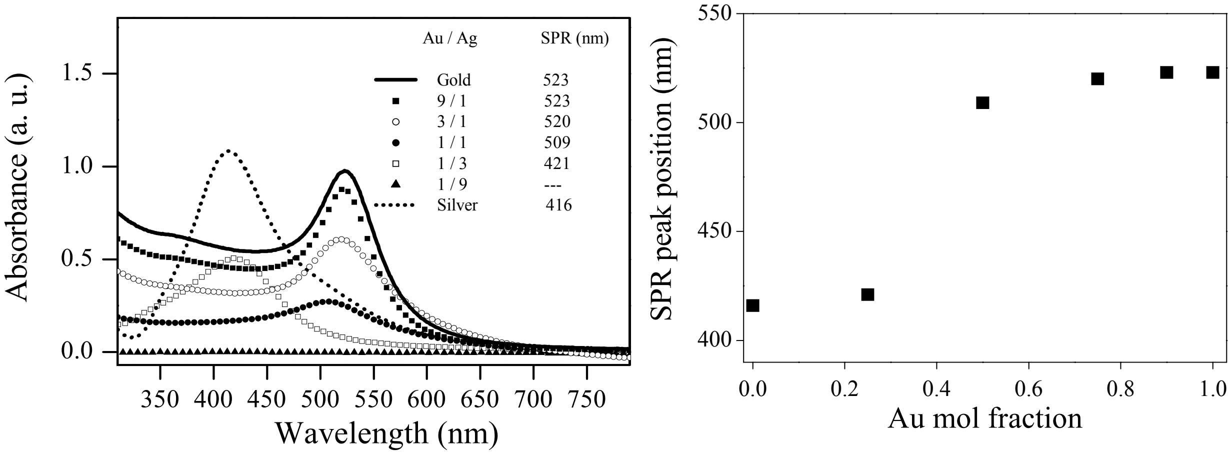

Figure 1. Optical absorption spectra of the bimetallic colloidal samples prepared at different Au/Ag molar ratios, using metal ion solutions of high concentrations (first set of metal ion solutions). The positions of the SPR peaks are plotted against Au mol fraction at the right.

Absorption spectra of the bimetallic colloids prepared with higher concentrations of metal ions (first set of metal ion solutions) are presented in figure 1. The monometallic dispersions of Au and Ag revealed absorption peaks at about 520 and 413 nm, respectively. While the SPR peaks for the bimetallic colloids prepared with Au/Ag = 9/1 and 3/1 appeared at the same position as that of monometallic Au, for the colloids with Au/Ag = 1/3, the SPR peak position appeared around 418 nm, which is very close to the SPR position of monometallic Ag. Appearance of no absorption peak in the case of Au/Ag =1/9 indicates the formation of neither type of nanoparticles. On the other hand, the SPR peak positions (Fig.1, right) of the colloidal solutions do not obey any linear or quasi-liner relationship with the Au mol fraction in the final reaction mixtures. These characteristics demonstrate that with the utilization of metal ion concentrations higher than the solubility product K_{ps} of AgCl(s), it is not possible to obtain Au/Ag alloy nanoparticles.

In figure 2, the absorption spectra of five bimetallic Au/Ag colloidal dispersions prepared with low concentration of metal ion solutions are presented. For comparison, absorption spectra of monometallic Au and Ag colloids are also presented. The peaks related to the SPR of Au and Ag particles were revealed at about 519 nm and 407 nm, which are consistent with the SPR peak positions of gold and silver nanoparticles, respectively [37]. There appeared only one absorption peak for each of the bimetallic colloids. The SPR absorption peaks for the bimetallic colloids are revealed in-between the SPR peak positions of monometallic Au and monometallic Ag colloids. Such absorption spectra can not be obtained either for the simple physical mixture of monometallic Au and Ag colloidal dispersions, or due to formation of core-shell Au-Ag nanoparticles, where there appear two characteristic absorption peaks [33,46]. The SPR peak position was blue-shifted in a quasi-linear fashion with an increasing Ag content due to the variation of composition of the bimetallic nanoparticles [37]. These observations strongly suggest

that each bimetallic particle is homogeneous Au/Ag alloy ones and the novel absorption bands are attributed to the SPR bands of Au-Ag alloy nanoparticles.

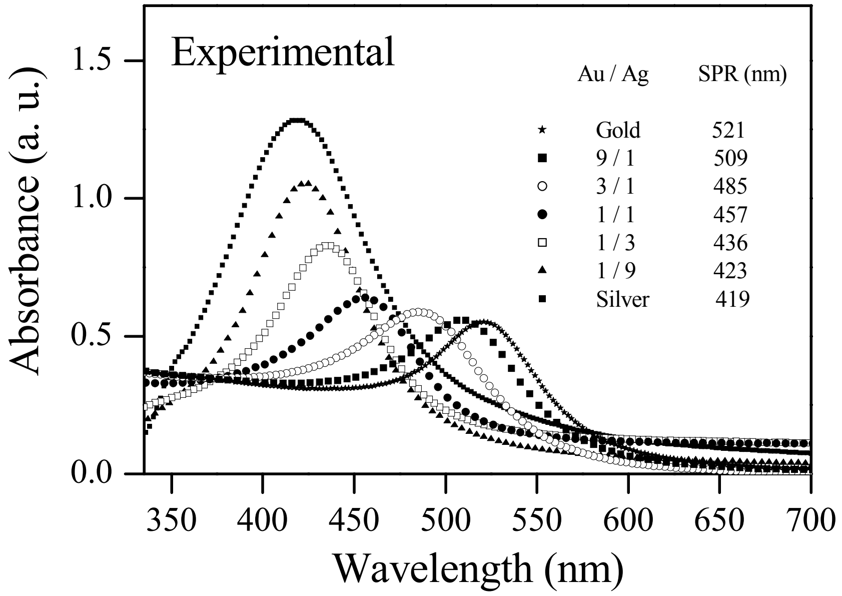

Figure 2. Optical absorption spectra of bimetallic colloids prepared with different Au/Ag molar ratios, using low metal ion concentrations (second set of metal ion solutions).

In figure 3, the experimentally obtained SPR peak positions are plotted against the molar ratios of Au and Ag in the reaction mixtures. A quasi-linear variation of the SPR peak position with Au mole fraction infers that the composition of the alloy colloids correspond to the initial concentrations of gold and silver ions in the reaction mixtures. On the other hand, the SPR peak positions of the colloids obtained from their theoretically calculated absorption spectra (presented latter) are also presented in figure 3 (open squares). Close resemblance of the theoretically obtained SPR position values with the corresponding experimentally obtained SPR peak positions indicates that the bimetallic nanoclusters are of true alloy character and of compositions very close to their nominal compositions. A similar variation of SPR peak position with the

variation of Au mole fraction in bimetallic alloy clusters has been observed by Peng et al. [26] for their Au-Ag colloids prepared by laser-assisted synthesis. Therefore, by controlling the initial concentrations of gold and silver ions in the reaction mixtures, we could control the SPR frequency of Au-Ag alloy nanoparticles. It must be noted that the variation of our SPR peak position calculated considering the bulk dielectric constants of Au and Ag is not exactly linear as observed by Link et al. [37] considering the dielectric constant of alloy thin film. However, the variation resembles extremely well with the experimentally observed variation. In the further parts of this article, we will discuss only on the second batch of samples (prepared with lower concentration of metal ions in the reaction mixture) for which nanoparticles of uniform composition were obtained.

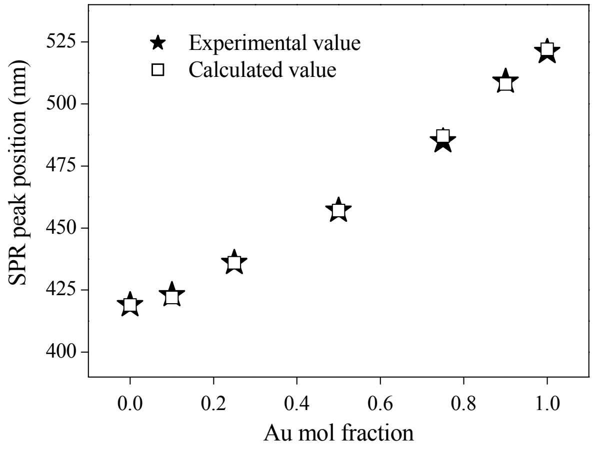

Figure 3. Relationship between Au content and surface plasmon resonance peak position of Au/Ag alloy nanoparticles (for the second set of metal ion solutions): (■) experimental and (□) calculated.

In order to determine the size of the nanoparticles, TEM analysis has been performed. In figure 4, typical TEM micrographs of the bimetallic nanoparticles prepared with different molar ratios of Au and Ag (Au/Ag = 9/1, 3/1, 1/1, 1/3 y 1/9) and their respective size distribution histograms are presented. For the histograms, the size of more than 60 particles was measured.

The images reveal the formation of nearly spherical nanometric particles. The average particle size varied from 19.4 to 43.2 nm depending on the concentrations of two metals in them. However, the size dispersion decreases with the increase of Au content in them. Absence of bimodal size distribution in the size distribution histograms suggests that the nanoparticles obtained by our synthesis process are not the simple mixture of monometallic particles of Au and Ag. The average particle size increased with the increase of Ag contents in bimetallic nanoparticles until about 75 %. Further increase of Ag content reduced the average diameter of the bimetallic nanoparticles. Dependence of particle size on composition for bimetallic nanoparticles has been studied by several researchers. Esumi et al. [47] and Wu et al. [48] have also observed a positive deviation of mean diameter for Pd/Pt bimetallic nanoparticles on composition.

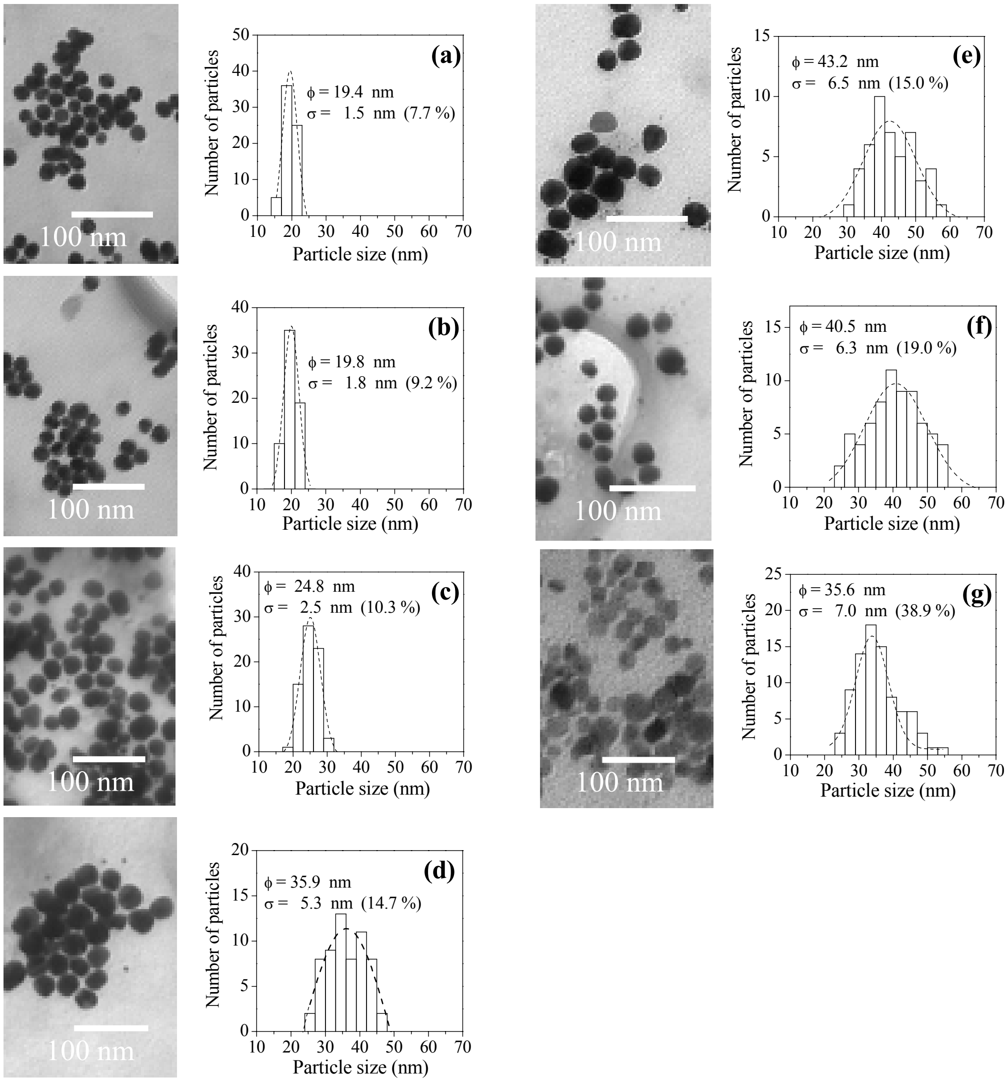

Figure 4. Typical TEM micrographs and corresponding size distribution histograms for the Au/Ag bimetallic nanoparticles (prepared using second set of metal ion solutions) with different molar ratios of Au/Ag: (a) 1/0, (b) 9/1, (c) 3/1, (d) 1/1, (e) 1/3, (f) 1/9 and (g) 0/1. Average particle size ϕ and standard deviation σ are calculated from the Gaussian fittings of the histograms.

The increase of particle size on increasing the Ag content in the bimetallic nanoparticles can be explained by considering the reduction velocity of the individual metal ions. As the reduction potential of Ag (0.8 V) is smaller that the reduction potential of Au (1.5 V), the velocity of reduction of Au ions is faster than the velocity of reduction of Ag ions. So, an increasing Ag ion content in the mixture solution inhibits the nucleation rate of the bimetallic nanoparticles and as consequence, the bimetallic particles grow bigger and dispersed [49].

For a closer observation on the crystallinity, composition and fine structure of the bimetallic nanoparticles, HREM images of two samples (Au/Ag = 1/1 and 1/3) were recorded. From the HREM images (Fig. 5), we can observe the formation of well crystalline multiple twined nanoparticles for both the samples. In fact most of the bimetallic nanoparticles formed in our bimetallic systems were multiple twined. The lattice spacings in the nanoparticles are clearly visible in the amplified images of the selected areas presented as insets. Inter-planer spacing calculated for both the samples correspond well with the inter-planer spacing of the corresponding alloy structures of fcc phase. However, due to a very similar lattice constant values of gold (0.408 nm) and silver (0.409 nm), it was not possible to confirm the alloy nature of the

particles with certainty from their HREM images. To confirm the compositional homogeneity of the nanoparticles we recorded the HAADF images of the alloy particles.

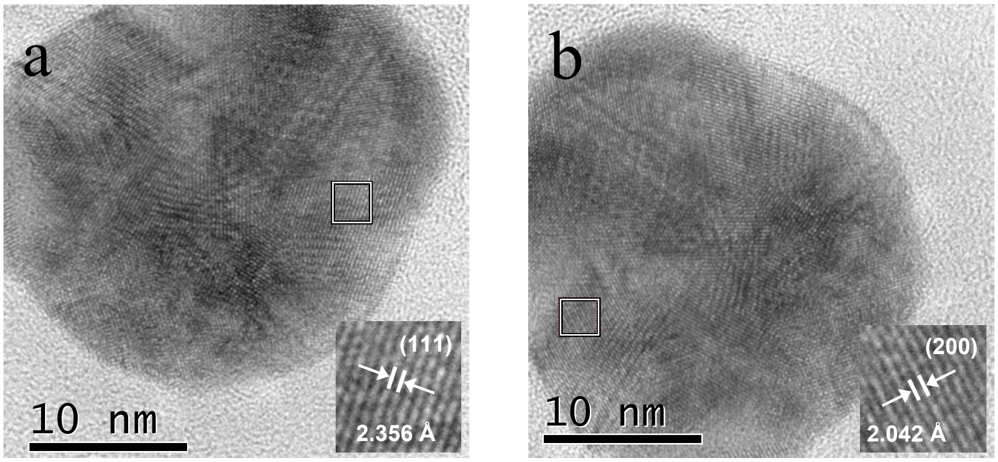

Figure 5. High-resolution electron micrographs of bimetallic colloidal particles a) Au/Ag = 1/1 and b) Au/Ag = 1/3 (prepared using second set of metal ion solutions). Amplified images of the marked portions are given as insets.

HAADF imaging uses high-angle scattered electrons to obtain spatially resolved images which are able to show suitable details about the compositional inhomogenity and structural characteristic of bimetallic nanoparticles. High-angle scattering is associated with electron interaction close to the nucleus of the atoms which constitute the sample (Rutherford scattering). So, the scattering phenomenon is strongly dependent on the atomic number (Z). The HAADF image contrast is proportional to the 1.7 power of the average atomic number in the atomic column. As the Z of Ag (47) and Au (79) are amply different, the Z-contrast imaging method should be able to determining the possible inhomogenity in chemical composition and structural conformation within the bimetallic nanoparticles. Figure 6 shows the typical HAADF images of our bimetallic nanoparticles prepared with Au/Ag = 1/1 and Au/Ag = 1/3 compositions. We can

perceive only a homogeneous image contrast for both the samples. No significant variation in contrast/intensity over the entire volume of the nanoparticles confirms a homogeneous distribution of metal atoms (Au and Ag) in them. In contrary, we could have observed HAADF images with inhomogeneous contrasts, as in the case of core-shell nanoparticles [51]. Therefore, the bimetallic nanoparticles obtained under the present synthesis conditions are of homogeneous solid-solution alloys of Au and Ag.

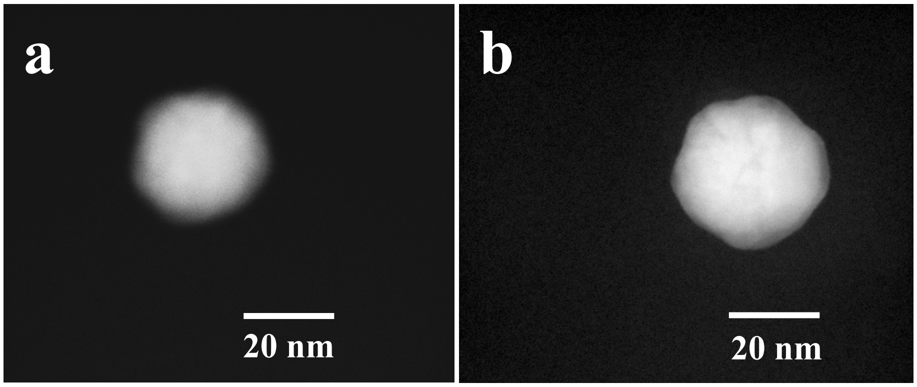

Figure 6. Typical HAADF images of a) Au/Ag (=1/1), and b) Au/Ag (= 1/3) bimetallic nanoparticles (prepared using second set of metal ion solutions) showing homogeneous elemental distribution.

To verify the composition of the nanoparticles, energy dispersive spectroscopy (EDS) analysis on the particles was carried out inside the transmission electron microscope for three sets of samples with compositions Au/Ag = 1/1, 1/3 and 1/9. We could not detect any particle of monometallic nature in them. Though the composition of individual particles varied from particle to particle for a given sample, the average composition remained close to its nominal value. The global composition of the samples was also monitored through EDS spectroscopy in a scanning electron microscope. In the figure 7, the EDS spectra of the samples Au/Ag = 1/1 and 3/1 are presented. Along with the Au and Ag emission peaks, there appeared carbon, oxygen and copper

emissions in the EDS spectra of the samples. While the origin of the carbon, oxygen and copper emissions are related to the carbon film on the grid surface, citrate salt, and copper micro-grid, respectively, the obtained Au/Ag atomic ratios for the samples fairly agree with their nominal molar ratios (Au/Ag = 1.05 and 3.02 for the samples prepared with nominal Au and Ag molar ratios of 1/1 and 3/1 respectively).

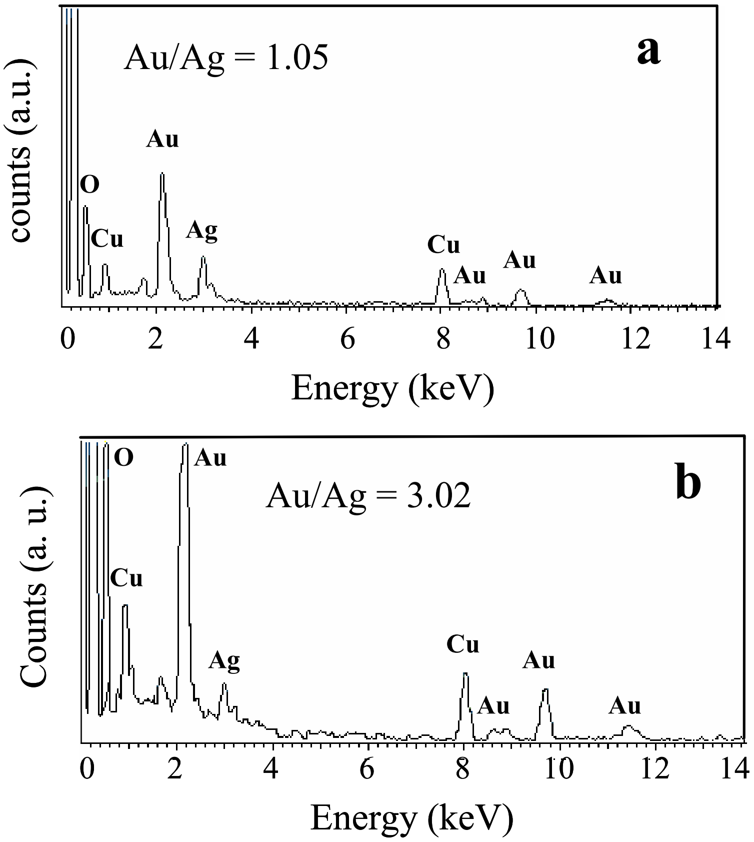

Figure 7. EDS spectra of the colloidal samples (prepared with second set of metal ion solutions) with nominal molar ratio a) Au/Ag = 1/1 and b) Au/Ag = 3/1.

Calculated optical absorption spectra of the colloids with different molar ratios of Au and Ag are presented in Figure 8. The shape, intensity and position of the SPR peak in our calculated absorption spectra were in close resemblance with the corresponding experimentally obtained

absorption spectra. The intensity of the SPR peak increases, and shifts toward shorter wavelengths with the increase of silver concentration.

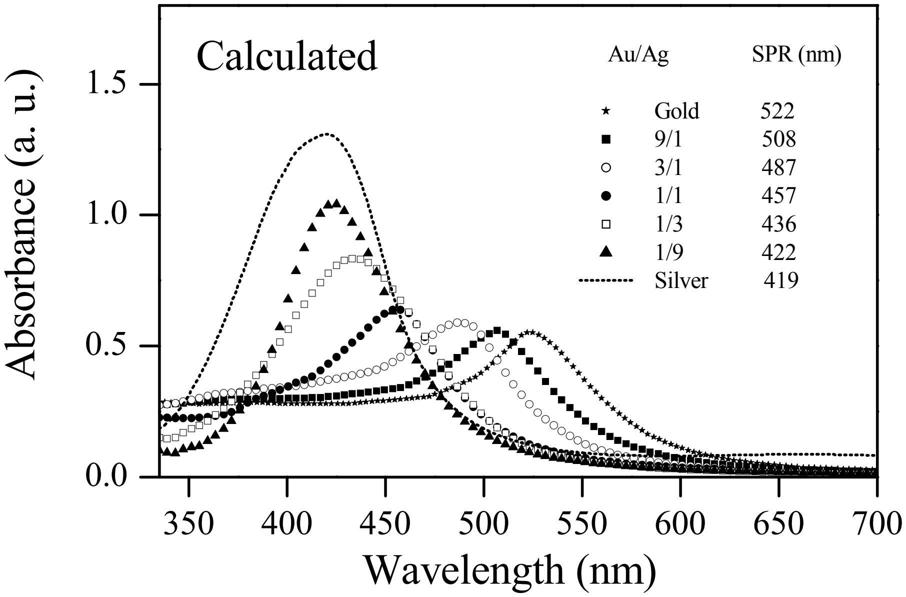

Figure 8. Calculated optical absorption spectra for Au-Ag bimetallic colloidal solutions with different molar ratios of Au and Ag.

Conclusions

Au-Ag nanoclusters of solid-solution alloy type could be prepared by simultaneous reduction of gold and silver ions using sodium citrate as reductor. For obtaining bimetallic clusters of true alloy type while using $HAuCl_4$ and $AgNO_3$ as precursors, the solubility product of the metal ion solutions should be kept below the solubility product (K_{ps}) of solid $AgCl_{(s)}$. On the contrary, chlorine ions from $HAuCl_4$ react with silver ions forming solid AgCl, inhibiting the formation of bimetallic alloy clusters. While the composition of the bimetallic alloy clusters could be maintained close to their nominal compositions, the SPR absorption band positions could be

tuned precisely close to their theoretical values. Considering true size distribution of the nanoparticles, and a modified Mie theory, the optical absorption spectra of the colloids could be reproduced theoretically. Bimetallic Au-Ag alloy nanoparticles of any composition can be prepared using our synthesis method.

Acknowledgements

Authors are thankful to VIEP-BUAP, CONACyT, and IPN, Mexico for their partial financial supports. We acknowledge the Central Microscopy Laboratory of IF-UNAM for extending TEM and HREM facilities.

References:

[1] J. F. Sánchez-Ramírez, J. L. Jiménez-Pérez, A. Cruz Orea, R. Gutierrez Fuentes, A. Bautista-Hernández, & U. Pal, "Thermal diffusivity of nanofluids containing Au/Pd bimetallic nanoparticles of different compositions" Journal of Nanoscience and Nanotechnology, Vol. 6, pp 685-690, 2006.

[2] R. Esparza, G. Rosas, M. López-Fuentes, J. F. Sánchez-Ramírez, U. Pal. J. A. Ascencio, & R. Pérez, "Synthesis of gold nanoparticles with different atomistic structural characteristics", Materials Characterization, Vol. 58, PP 694-700, 2007.

[3] J. F. Sánchez-Ramírez, C. Vázquez-López, & U. Pal, "Preparation and optical absorption of colloidal dispersion of Au/Cu nanoparticles", Superficies y Vacio, Vol. 15, pp 16-18, 2002.

[4] J. L. Rodríguez-López, J. M. Montejano Carrizales, U. Pal, J. F. Sánchez-Ramírez, H. Troiani, D. García, M. Miki-Yoshida, & M. José-Yacaman, "Surface Reconstruction and Decahedral Structure of Bimetallic Nanoparticles", Physical Review Letters, Vol. 92, P 196102, 2004.

[5] R. Kubo, "Electronic Properties of Metallic Fine Particles I", Journal of Physical Society of Japan, Vol. 17, pp 975-986, 1962.

[6] M.O. Nutt, K. N. Heck, P. Alvarez, and M. S. Wong, "Improved Pd-on-Au bimetallic nanoparticle catalysts for aqueous-phase trichloroethene hydrodechlorination", Applied Catalysis B, Vol. 69, pp 115-125, 2006.

[7] T. Ishii, H. Otsuka, K. Kataoka, & Y. Nagasaki, "Preparation of Functionally PEGylated Gold Nanoparticles with Narrow Distribution through Autoreduction of Auric Cation by α-Biotinyl-PEG-block-[poly(2-(N,N-dimethylamino)ethyl methacrylate)]", Langmuir, Vol. 20, pp 561-564, 2004.

[8] A. Sarkar, S. Kapoor, & T. Mukherjee, "Preparation, Characterization, and Surface Modification of Silver Nanoparticles in Formamide", Journal of Physical Chemistry B, Vol. 109, pp 7698-7704, 2005.

[9] H. Ye, and R. M. Crooks, "Effect of Elemental Composition of PtPd Bimetallic Nanoparticles Containing an Average of 180 Atoms on the Kinetics of the Electrochemical Oxygen Reduction Reaction", Journal of American Chemical Society, Vol. 129, pp 3627-3633, 2007.

[10] P. Hernández-Fernández, S. Rojas, P. Ocón, D. L. Gómez de la Fuente, J. San Fabián, J. Sanza, M. A. Peña, F. J. García-García, P. Terreros, J. L. G. Fierro, "Influence of the Preparation Route of Bimetallic Pt-Au Nanoparticle Electrocatalysts for the Oxygen Reduction Reaction", Journal of Physical Chemistry C, Vol. 111, pp 2913-2923, 2007.

[11] A. K. Sharma, and B. D. Gupta, "Fibre-optic sensor based on surface plasmon resonance with Ag–Au alloy nanoparticle films", Nanotechnology, Vol. 17, pp 124-131, 2006.

[12] L. Jun-Hong, W. Ai-Qin, C. Yu-Shan, L. Hong-Ping, & M. Chung-Yung, "Synergistic Effect in an Au-Ag Alloy Nanocatalyst: CO Oxidation", Journal of Physical Chemistry B, Vol. 109, pp 40-43, 2005.

[13] C. Burda, X. Chen, R. Narayanan, and M. A. El-Sayed, "Chemistry and Properties of Nanocrystals of Different Shapes", Chemical Review, Vol. 105, pp 1025-1102, 2005.

[14] S. A. Zynio, A. V. Samoylov, E. R. Surovtseva, V. M. Mirsky, & Y. M. Shirshov, "Bimetallic Layers Increase Sensitivity of Affinity Sensors Based on Surface Plasmon Resonance", Sensors, Vol. 2, pp 62-70, 2002.

[15] R. Basnayake, Z. Li, S. Katar, W. Zhou, H. Rivera, E. S. Smotkin, D. J. Jr. Casadonte, and C. Korzeniewski, "PtRu Nanoparticle Electrocatalyst with Bulk Alloy Properties Prepared through a Sonochemical Method" Langmuir, Vol. 22, pp 10446-10450, 2006.

[16] A. M. Molenbroek, S. Haukka, and B. S. J. Clausen, "Alloying in Cu/Pd Nanoparticle Catalysts", Journal of Physical Chemistry B, Vol. 102, pp 10680-10689, 1998.

[17] L. Seol-Ah, P. Kyung-Won, C. Jong-Ho, K. Boo-Kil, & S. Yung-Eun, "Nanoparticle Synthesis and Electrocatalytic Activity of Pt Alloys for Direct Methanol Fuel Cells", Journal of Electrochemical Society, Vol. 149, p A1299, 2002.

[18] W. Ai-Qin, L. Jun-Hong, S.D. Lin, L. Tien-Sung, M. Chung-Yuan, "A novel efficient Au–Ag alloy catalyst system: preparation, activity, and characterization", Journal of Catalysis, Vol. 233, pp 186-197, 2005.

[19] R. Esparza, J. A. Ascencio, G. Rosas, J. F. Sánchez-Ramírez, U. Pal, and R. Pérez Campos, "Structure, Stability and Catalytic Activity of Chemically Synthesized Pt, Au, and Au–Pt Nanoparticles", Journal of Nanoscience and Nanotechnology, Vol. 5, pp 641-647, 2005.

[20] L. Jun-Hong, W. Ai-Qin, C. Yu-Shan, C. Yu-Shan, L. Hong-Ping, and M. Chung-Yung, "Synergistic Effect in an Au-Ag Alloy Nanocatalyst: CO Oxidation", Journal of Physical Chemistry B, Vol. 109, pp 40-43, 2005.

[21 N. K. Chaki, H. Tsunoyama, Y. Negishi, H. Sakurai, and T. Tsukuda, "Effect of Ag-Doping on the Catalytic Activity of Polymer-Stabilized Au Clusters in Aerobic Oxidation of Alcohol", Journal of Physical Chemistry C, Vol. 111, pp 4885-4888, 2007.

[22 K. Kim, K.L. Kim, and S.J. Lee, "Surface enrichment of Ag atoms in Au/Ag alloy nanoparticles revealed by surface enhanced Raman scattering spectroscopy", Chemical Physics Letters, Vol. 403, pp 77-82, 2005.

[23 Q. Zhang, J. Y. Lee, J. Yang, C. Boothroyd, and J. Zhang, "Size and composition tunable Ag–Au alloy nanoparticles by replacement reactions", Nanotechnology, Vol. 18, p 45605, 2007.

[24 S. Senapati, A. Ahmad, M. I. Khan, M. Sastry, and R. Kumar, “Extracellular Biosynthesis of Bimetallic Au-Ag Alloy Nanoparticles”, Small, Vol. 1, pp 517-520, 2005.

[25 P. Raveendran, J. Fu, and S. L. Wallen, “A simple and green method for the synthesis of Au, Ag, and Au–Ag alloy nanoparticles”, Green Chemistry, Vol. 8, pp 34-38, 2006.

[26 Z. Peng, B. Spliethoff, B. Tesche, T. Walther, and K. J. Kleinermanns, “Laser-Assisted Synthesis of Au-Ag Alloy Nanoparticles in Solution”, Journal of Physical Chemistry B, Vol. 110, pp 2549-2554, 2006.

[27 B. Karthikeyan, M. Anija, and R. Philip, “In situ synthesis and nonlinear optical properties of Au:Ag nanocomposite polymer films”, Applied Physics Letters, Vol. 88, p 053104, 2006.

[28 H. M. Chen, R. S. Liu, L. Y. Jang, J. F. Lee, and S. F. Hu, “Characterization of core–shell type and alloy Ag/Au bimetallic clusters by using extended X-ray absorption fine structure spectroscopy”, Chemical Physics Letters, Vol. 421, pp 118-123, 2006.

[29] I. Lee, S. W. Han, and K. Kim, “Production of Au–Ag alloy nanoparticles by laser ablation of bulk alloys”, Chemical Communications, Vol. 18, pp 1782-1783, 2001.

[30 H. Takatani, H. Kago, M. Nakanishi, Y. Kobayashi, F. Hori, and R. Oshima, “Characterization of Noble Metal Alloy Nanoparticles Prepared by Ultrasound Irradiation”, Reviews on Advanced Materials Science, Vol. 5, pp 232-238, 2003.

[31 A. A. Schmidt, and R. Anton, “Anomalous growth behaviour of Pd-Au and Ag-Au alloy particles during vapour deposition on carbon substrates at elevated temperatures”, Surface Science, Vol. 322, pp 307-324, 1995.

[32 C. S. Ah, S. D. Hong, and D. Jang, “Preparation of $Au_{core}Ag_{shell}$ Nanorods and Characterization of Their Surface Plasmon Resonances”, Journal of Physical Chemistry B, Vol. 105, pp 7871-7873, 2001.

[33 K. Mallik, M. Mandal, N. Pradhan, and T. Pal, “Seed Mediated Formation of Bimetallic Nanoparticles by UV Irradiation: A Photochemical Approach for the Preparation of "Core-Shell" Type Structures”, Nano Letters, Vol. 1, pp 319-322, 2001.

[34 L. Rivas, S. Sánchez-Cortes, J.V. García-Ramos, and G. Morcillo, “Mixed Silver/Gold Colloids: A Study of Their Formation, Morphology, and Surface-Enhanced Raman Activity”, Langmuir, Vol. 16, pp 9722-9728, 2000.

[35 S. Mandal, P. R. Selvakannan, R. Pasricha, and M. Sastry, “Keggin Ions as UV-Switchable Reducing Agents in the Synthesis of Au Core-Ag Shell Nanoparticles”, Journal of American Chemical Society, Vol. 125, pp 8440-8441, 2003.

[36 L. Lu, H. Wang, Y. Zhou, S. Xi, H. Zhang, J. Hu, and B. Zhao, “Seed-mediated growth of large, monodisperse core–shell gold–silver nanoparticles with Ag-like optical properties”, Chemical Communications, Vol. 2, pp 144-145, 2002.

[37] S. Link, Z. L. Wang, and M. A. El-Sayed, “Alloy Formation of Gold-Silver Nanoparticles and the Dependence of the Plasmon Absorption on Their Composition” Journal of Physical Chemistry B, Vol. 103, pp 3529-3533, 1999.

[38] Z. Peng, B. Spliethoff, B. Tesche, T. Waltherm, and K. Kleinermanns, “Laser-Assisted Synthesis of Au-Ag Alloy Nanoparticles in Solution”, Journal of Physical Chemistry B, Vol. 110, pp 2549-2554, 2006.

[39] U. Kreibing, and M. Vollmer, “Optical Properties of Metal Clusters”, Vol 25, (ed) Springer, Verlag Berlin Heidelberg New York, 1995.

[40] C. F. Bohren, and D. R. Huffman, “Absorption and Scattering of Light by Small Particles (ed) Wiley, New York, 1998.

[41] P. Mulvaney, “Surface Plasmon Spectroscopy of Nanosized Metal Particles”, Langmuir, Vol. 12, pp 788-800, 1996.

[42] P. B. Johnson, and R. W. Cristy, “Optical Constants of the Noble Metals”, Physical Review B, Vol. 6, pp 4370-4374, 1972.

[43] M. Bernhard, and L. Eberhard, “MieCalc - freely configurable program for light scattering calculations (Mie theory)”, 2006, http://www.lightscattering.de/MieCalc/eindex.html.

[44] R.C. Weast, M. J. Astle, and W. H. Beyer, Eds. “CRC Handbook of Chemistry and Physics” 65th edn. CRC Press, Inc. Boca Raton, FL, 1984.

[45] M. A. El-Sayed, “Some Interesting Properties of Metals Confined in Time and Nanometer Space of Different Shapes”, Accounts of Chemical Research, Vol. 34, pp 257-264, 2001.

[46] M. Liu, and P. Guyot-Sionnest, “Synthesis and Optical Characterization of Au/Ag Core/Shell Nanorods”, Journal of Physical Chemistry B, Vol. 108, pp 5882-5888, 2004.

[47] K. Esumi, M. Shiratori, H. Ishizuka, H. Ishizuka, T. Tano, K. Torigoe, and K. Meguro, “Preparation of bimetallic palladium-platinum colloids in organic solvent by solvent extraction-reduction”, Langmuir, Vol. 7, pp 457-459, 1991.

[48] M. L. Wu, D. H. Chen, and T. C. Huang, “Preparation of Pd/Pt Bimetallic Nanoparticles in Water/AOT/Isooctane Microemulsions”, Journal of Colloidal and Interface Science, Vol. 243, pp 102-108, 2001.

[49] D. H. Chen, and C. J. Chen, “Formation and characterization of Au–Ag bimetallic nanoparticles in water-in-oil microemulsions", Journal of Materials Chemistry, Vol. 12, pp 1557-1562, 2002.

[50] D. Garcia-Gutierrez, C. Gutierrez-Wing, M. Miki-Yoshida, and M. Jose-Yacaman, "HAADF study of Au-Pt core-shell bimetallic nanoparticles", Applied Physics A, Vol. 79, pp 481-487, 2004.

Figure and Table captions:

Table 1. Concentrations, f values and bulk free electron gas parameters for Au/Ag alloys of different compositions.

Figure 1. Optical absorption spectra of the bimetallic colloidal samples prepared at different Au/Ag molar ratios, using metal ion solutions of high concentrations (first set of metal ion solutions). The positions of the SPR peaks are plotted against Au mol fraction at the right.

Figure 2. Optical absorption spectra of bimetallic colloids prepared with different Au/Ag molar ratios, using low metal ion concentrations (second set of metal ion solutions).

Figure 3. Relationship between Au content and surface plasmon resonance peak position of Au/Ag alloy nanoparticles (for the second set of metal ion solutions): (■) experimental and (□) calculated.

Figure 4. Typical TEM micrographs and corresponding size distribution histograms for the Au/Ag bimetallic nanoparticles (prepared using second set of metal ion solutions) with different molar ratios of Au/Ag: (a) 1/0, (b) 9/1, (c) 3/1, (d) 1/1, (e) 1/3, (f) 1/9 and (g) 0/1. Average particle size ϕ and standard deviation σ are calculated from the Gaussian fittings of the histograms.

Figure 5. High-resolution electron micrographs of bimetallic colloidal particles a) Au/Ag = 1/1 and b) Au/Ag = 1/3 (prepared using second set of metal ion solutions). Amplified images of the marked portions are given as insets.

Figure 6. Typical HAADF images of a) Au/Ag (=1/1), and b) Au/Ag (= 1/3) bimetallic nanoparticles (prepared using second set of metal ion solutions) showing homogeneous elemental distribution.

Figure 7. EDS spectra of the colloidal samples (prepared with second set of metal ion solutions) with nominal molar ratio a) Au/Ag = 1/1 and b) Au/Ag = 3/1.

Figure 8. Calculated optical absorption spectra for bimetallic colloidal solutions with different molar ratios of Au and Ag.